J Therm Anal Calorim (2011) 103:141–145
DOI 10.1007/s10973-010-1076-2

Thermodynamic description of the Ru–Y binary system

**M. Ait Amar · M. Idbenali · N. Selhaoui ·
K. Mahdouk · A. Aharoune · L. Bouirden**

Received: 2 July 2010 / Accepted: 22 September 2010 / Published online: 9 October 2010

Abstract The thermodynamic modeling of the Ruthenium–Yttrium binary system was carried out with the help of CALPHAD (CALculation of PHAse Diagram) method. Ru_2Y, Ru_2Y_3, $Ru_{25}Y_{44}$, Ru_2Y_5, and RuY_3 have been treated as stoichiometric compounds while a solution model has been used for the description of the liquid, BCC_A2, and HCP_A3 phases. The calculations based on the thermodynamic modeling are in good agreement with the phase diagram data and experimental thermodynamic values available in the literature.

Keywords Ru–Y system · Phase diagram · Thermodynamic description · CALPHAD method

Introduction

This study is a part of a thermodynamic investigation of the Ru–R systems (R=Zr…) [1] which is intended to give a better understanding of the constitutional properties and potential technological applications of these alloys.

This study deals with an assessment of the thermodynamic description of the Ru–Y system using the CALPHAD method [2]. The thermodynamic parameters involved in the models are optimized from the experimental thermodynamic and phase diagram data.

Experimental information

The first study of the phase diagram Ru–Y is due to Savitsky et al. [3], who reported only two compounds Ru_2Y and RuY_3. After that, Sharifrazi et al. [4] found two others compounds Ru_2Y_3 and Ru_2Y_5. Fornasini et al. [5] carried out detailed crystal studies and reported that “Ru_3Y_5” should be $Ru_{25}Y_{44}$.

The currently accepted Ru–Y phase diagram Fig. 1 is based on an investigation carried out by Massalski [6]. The equilibrium phases include: (1) the liquid; (2) five intermediates phases Ru_2Y, Ru_2Y_3, $Ru_{25}Y_{44}$, Ru_2Y_5, and RuY_3; and (3) the two terminal solid phases: HCP_A3 and BCC_A2. The crystal structures of various phases are reported in Table 1.

For the Ru_2Y and Ru_2Y_5 compounds, a congruent melting was estimated, respectively, at 2223 and 1593 K, while for the Ru_2Y_3, $Ru_{25}Y_{44}$, and RuY_3 compounds, a peritectic formation was reported, respectively, at 1623, 1568, and 1523 K.

Selhaoui and Kleppa [7, 8] measured the standard enthalpies of formation of Ru_2Y and Ru_2Y_5 by direct reaction calorimetry at high temperature. The values obtained are, respectively, -19.5 ± 1.4 and -27.3 ± 3.1 kJ mol^{-1} at^{-1}. Selhaoui et al. [9] attempted to assess the phase diagram using the NancyUn software elaborated by Charles et al. [10, 11]. This routine is less powerful than the Thermo Calc software [12] because, it took into account only the liquid and intermetallic phases but neither the terminal solid

---

It was presented at JEEP2010 Montpellier, France.

M. Ait Amar (✉) · M. Idbenali · N. Selhaoui · K. Mahdouk ·
A. Aharoune · L. Bouirden
Laboratory of Thermodynamics and Energy (L.T.E.),
Faculty of Science, University Ibn Zohr,
B.P. 8106 Agadir, Morocco
e-mail: amar.amarmed@gmail.com

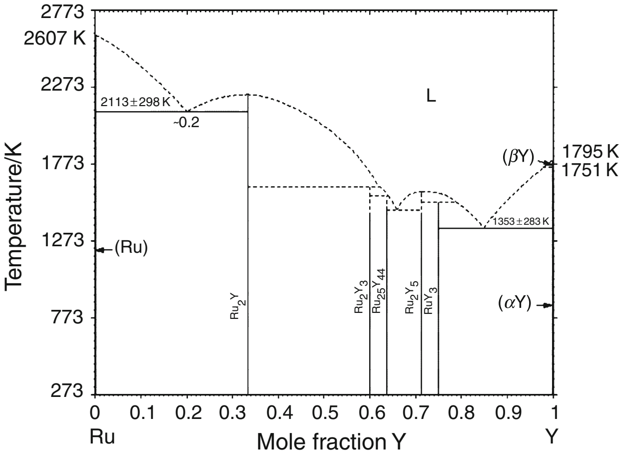

Fig. 1 Experimental Ru–Y phase diagram previously published by Massalski [6]

Table 1 Symbols and crystal structures of the stable solid phases in the Ru–Y system [6]

Diagram symbol	Composition/ at.% Y	Pearson symbol	Symbol used in thermo-calc data file	Prototype
Ru	0	hP2	HCP_A3	Mg
βY	100	cI2	BCC_A2	W
αY	100	hP2	HCP_A3	Mg
RuY_3	75	oP16	RuY_3	CFe_3
Ru_2Y_5	71.42	mS28	Ru_2Y_5	C_2Mn_5
Ru_2Y_3	60	hP2	Ru_2Y_3	Ru_2Er_3
Ru_2Y	33.33	hP2	Ru_2Y	Zn_2Mg
$Ru_{25}Y_{44}$	63.76	oP276	$Ru_{25}Y_{44}$	$Ru_{25}Y_{44}$

phases BCC_A2 and HCP_A3 nor the (αY) and (βY) transitions are considered by NancyUn.

Thermodynamic models

Unary Phases

The Gibbs energy function $G_i^{\varphi}(T) = {}^0G_i^{\varphi} - H_i^{\mathrm{SER}}$ (298.15 K) for the element i (i = Ru, Y) in the phase φ (φ = Liquid, BCC_A2, or HCP_A3) is described by an equation of the following form:

$$G_i^{\varphi}(T) = a + bT + cT\ln T + dT^2 + eT^3 + fT^7 + gT^{-1} + hT^{-9},$$

where H_i^{SER}(298.15 K) is the molar enthalpy of the element i at 298.15 K in its standard element reference (SER) state, HCP_A3 for Ru and Y.

In this article, the Gibbs energy functions are taken from the Scientific Group Thermodata Europe (SGTE) compilation by Dinsdale [13].

Solution phases

The solution phase liquid was modeled as substitution solution. The Gibbs energy of 1 mol of formula unit of phase φ is expressed as the sum of the reference part ${}^{\mathrm{ref}}G^{\varphi}$, the ideal part ${}^{\mathrm{id}}G^{\varphi}$, and the excess part ${}^{\mathrm{exc}}G^{\varphi}$: $G_m^{\varphi} = {}^{\mathrm{ref}}G^{\varphi} + {}^{\mathrm{id}}G^{\varphi} + {}^{\mathrm{exc}}G^{\varphi}$.

As used in the Thermo-calc software [12]:

$$\begin{aligned} {}^{\mathrm{ref}}G^{\varphi}(T) &= \left({}^0G_{\mathrm{Ru}}^{\varphi}(T) - H_{\mathrm{Ru}}^{\mathrm{SER}}(298.15)\right)x_{\mathrm{Ru}} \\ &\quad + \left({}^0G_{\mathrm{Y}}^{\varphi}(T) - H_{\mathrm{Y}}^{\mathrm{SER}}(298.15)\right)x_{\mathrm{Y}}, \end{aligned}$$

$${}^{\mathrm{id}}G^{\varphi} = RT(x_{\mathrm{Ru}}\ln x_{\mathrm{Ru}} + x_{\mathrm{Y}}\ln x_{\mathrm{Y}})$$

where R is the gas constant; T is temperature, in Kelvin; x_{Ru} and x_{Y} are the mole fractions of elements Ru and Y, respectively.

The excess terms of all the solution phases were modeled by the Redlich–Kister [14] formula:

Table 2 Thermodynamic parameters of the Ru–Y system in SI units

Liq	${}^0L^{\mathrm{liq}} = -102247 + 7.5T$
	${}^1L^{\mathrm{liq}} = 94183 - 45.5T$
	${}^2L^{\mathrm{liq}} = 65656 - 28.6T$
BCC_A2	No excess term
HCP_A3	${}^0L^{\mathrm{hcp}} = 28000$
Ru_2Y	$G_m^{\mathrm{Ru_2Y}} - 0.667G_{\mathrm{Ru}}^{\mathrm{hcp}} - 0.33G_{\mathrm{Y}}^{\mathrm{hcp}} = -20888 - 3.8T$
Ru_2Y_3	$G_m^{\mathrm{Ru_2Y_3}} - 0.4G_{\mathrm{Ru}}^{\mathrm{hcp}} - 0.6G_{\mathrm{Y}}^{\mathrm{hcp}} = -24789 + 0.001T$
$Ru_{25}Y_{44}$	$G_m^{\mathrm{Ru_{25}Y_{44}}} - 0.362G_{\mathrm{Ru}}^{\mathrm{hcp}} - 0.638G_{\mathrm{Y}}^{\mathrm{hcp}} = -25431 + 0.83T$
Ru_2Y_5	$G_m^{\mathrm{Ru_{25}Y_5}} - 0.286G_{\mathrm{Ru}}^{\mathrm{hcp}} - 0.714G_{\mathrm{Y}}^{\mathrm{hcp}} = -26844 + 2.9T$
RuY_3	$G_m^{\mathrm{RuY_3}} - 0.25G_{\mathrm{Ru}}^{\mathrm{hcp}} - 0.75G_{\mathrm{Y}}^{\mathrm{hcp}} = -23319 + 2T$

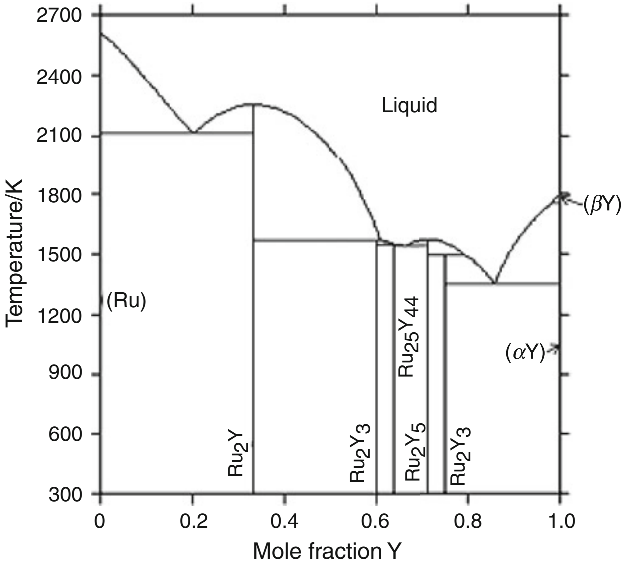

Fig. 2 The Ru–Y phase diagram calculated in the present work

$$
{}^{\mathrm{exc}}G_m^{\varphi}(T) = x_{\mathrm{Ru}}x_{\mathrm{Y}}\Big[{}^{0}L^{\varphi}_{(\mathrm{Ru,Y})}(T) + {}^{1}L^{\varphi}_{(\mathrm{Ru,Y})}(T)(x_{\mathrm{Ru}} - x_{\mathrm{Y}}) + {}^{2}L^{\varphi}_{(\mathrm{Ru,Y})}(T)(x_{\mathrm{Ru}} - x_{\mathrm{Y}})^2 + \cdots\Big],
$$

where ${}^{i}L^{\varphi}_{\mathrm{Ru,Y}}(T) = a_i + b_iT$ are the interaction parameters between the elements Ru and Y, which are evaluated in this study, T is the temperature in Kelvin and the coefficients a_i and b_i are optimized using the PARROT module [12], while x_{Ru} and x_{Y} are the mole fractions of elements Ru and Y, respectively.

Stoichiometric compounds

The Gibbs energy of the stoichiometric compound $\mathrm{Ru}_p\mathrm{Y}_q$, ${}^{0}G_{\mathrm{Ru}_p\mathrm{Y}_q}$, is expressed as follows:

$$
{}^{0}G_{\mathrm{Ru}_p\mathrm{Y}_q} = \frac{p}{p+q}{}^{0}G_{\mathrm{Ru}} + \frac{p}{p+q}{}^{0}G_{\mathrm{Y}} + a + bT,
$$

where ${}^{0}G_{\mathrm{Ru}}$ and ${}^{0}G_{\mathrm{Y}}$ are the Gibbs energy of the pure elements Ru and Y, respectively; a and b are parameters to be determined; T is temperature in Kelvin.

Optimization and discussions

Most of the experimental information mentioned above is selected in this study. The optimization is carried out by means of the Thermo-Calc software [12] which can take various kinds of experimental data.

The program works by minimizing an error sum where each of the selected data values are given a certain weight. The weight is chosen by personal judgment and changed by trial and error during the work until most of the selected experimental information is reproduced within the expected uncertainty limits. No enthalpy of mixing of the liquid was available in the literature. In the present parameter optimization procedure, we first imposed the conditions d^2G/dx^2 for modeling the liquid phase (${}^{0}L_{\mathrm{Ru,Y}}$) using the phase boundary data reported by Massalski [6] and thermodynamic data determined by Selhaoui and Kleppa [7, 8]. The thermodynamic parameters for the intermediate and liquid phases were optimized at the first stage based on the enthalpies of formation of the intermetallic compounds measured by Selhaoui and Kleppa [7, 8] and the invariant equilibrium from [6] by imposing additional constraints to avoid the appearance of unwanted inverted miscibility gap in the liquid phase during the phase diagram calculation as

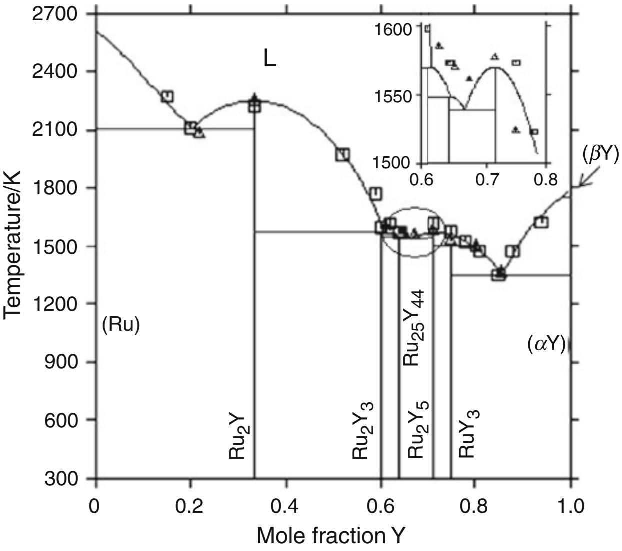

Fig. 3 Calculated Ru–Y phase diagram in the present work, *triangles* indicate the points taken from optimization by Selhaoui et al. [9] and *rectangles* indicate the experimental or estimated points taken from Massalski [6]

Table 3 Comparison between experimental data, calculated values by Selhaoui et al. [9] and optimized values in the present work of compositions of the liquid and temperatures for the invariant points

Reaction	Experimental[a] and estimates[b] values taken from Massalski [6]		Calculated by Selhaoui et al. [9]		Present work	
	T/K	x_{liq}/at.% Y	T/K	x_{liq}/at.% Y	T/K	x_{liq}/at.% Y
Liq ↔ Ru + $\mathrm{Ru_2Y}$	2113[a]	~20.00[a]	2081	20.70	2111	20.04
Liq ↔ $\mathrm{Ru_2Y}$	2223[b]	33.33	2253	33.33	2253	33.33
Liq + $\mathrm{Ru_2Y}$ ↔ $\mathrm{Ru_2Y_3}$	1623[b]	61.90[b]	1585	62.00	1570	60.86
Liq + $\mathrm{Ru_2Y_3}$ ↔ $\mathrm{Ru_{25}Y_{44}}$	1568[b]	64.10[b]	1570	64.70	1548	64.08
Liq ↔ $\mathrm{Ru_{25}Y_{44}}$ + $\mathrm{Ru_2Y_5}$	1473[b]	66.00[b]	1561	67.10	1539	66.39
Liq ↔ $\mathrm{Ru_2Y_5}$	1593[b]	71.42	1577	71.42	1570	71.42
Liq + $\mathrm{Ru_2Y_5}$ ↔ $\mathrm{RuY_3}$	1523[b]	78.95[b]	1493	80.40	1494	79.20
Liq ↔ $\mathrm{RuY_3}$ + αY	1353[a]	85.00[a]	1364	85.50	1353	85.79
βY ↔ Liq + αY	1751[b]	98.50[b]	–	–	1750	98.50

[a] Cited values in Massalski's phase diagram [6]

[b] Estimated values from Massalski's phase diagram [6]

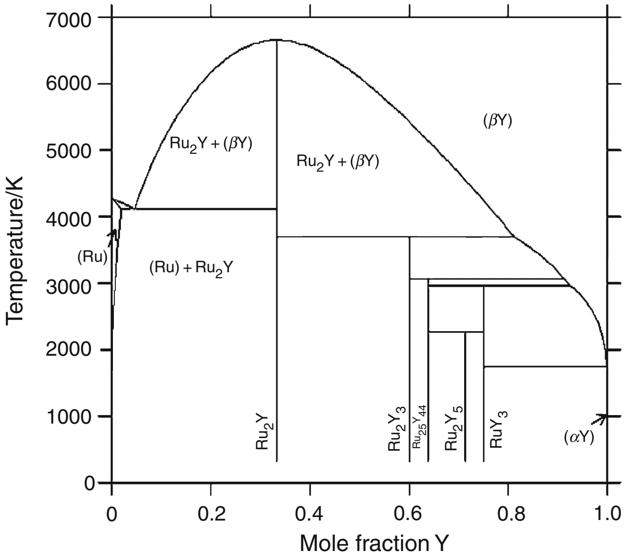

Fig. 4 Calculated Ru–Y phase diagram when the liquid phase is suspended

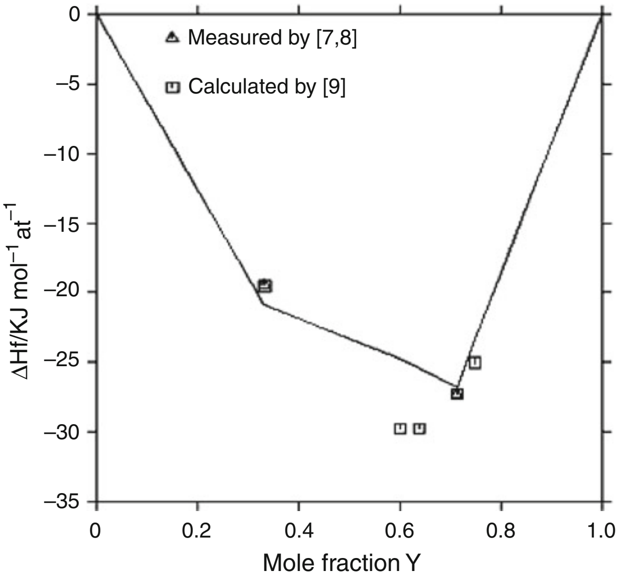

Fig. 5 The calculated enthalpy of formation in the Ru–Y with data values measured and calculated by Selhaoui et al. [7–9]

recommended in [15–17]. All the parameters were evaluated and listed in Table 2.

The Ru–Y phase diagram calculated from our optimized thermodynamic parameters is plotted in Fig. 2. It is compared with the numerous experimental data in Fig. 3. A satisfactory agreement is noted. The calculated invariant reactions of the Ru–Y system are listed in Table 3 and compared with the experimental results from [6] and optimized results in [9]. They are in reasonable agreement except for the temperature (1539 K) of Liq ↔ $Ru_{25}Y_{44}$ + Ru_2Y_5 invariant for which our result is different from the one estimated (1473 K) by Massalski [6]. However, this result is near from the one calculated by Selhaoui et al. [9]. We note that experimental part of the phase diagram is still uncertain.

As mentioned above the Gibbs energy of stoichiometric compound is expressed as follows: $G = a + bT$ with $a = H$ the enthalpy and $S = -b$ the entropy. In order to check that the optimized thermodynamic parameters of the intermetallic compounds are satisfactory, we verified two criteria:

- First: b must be between -10 and $+10$ J mol^{-1} K^{-1}.
- Second: the compounds should not be stable at high temperature compared to terminal solid phases, when the liquid phase is suspended as first stated by Chen et al. [15]. Indeed, we verified that, when the liquid phase is suspended during the calculation of the Ru–Y phase diagram, the stoichiometric phases disappear at

Table 4 Calculated and measured enthalpies of formation of the intermetallic compounds (referred to solid Ru and αY)

Phase	Enthalpy of formation/ kJ mol^{-1} at^{-1}	Technique used	Temperature/K	Reference
Ru_2Y	−19.500 ± 1.4	High temperature drop calorimetry	298	[7, 8]
	−19.530	Optimization	300	[9]
	−20.888	Optimization	300	This work
Ru_2Y_3	−29.177	Optimization	300	[9]
	−24.789	Optimization	300	This work
$Ru_{25}Y_{44}$	−29.778	Optimization	300	[9]
	−25.431	Optimization	300	This work
Ru_2Y_5	−27.300 ± 3.1	High temperature drop calorimetry	298	[7, 8]
	−27.288	Optimization	300	[9]
	−26.844	Optimization	300	This work
RuY_3	−25.052	Optimization	300	[9]
	−23.319	Optimization	300	This work

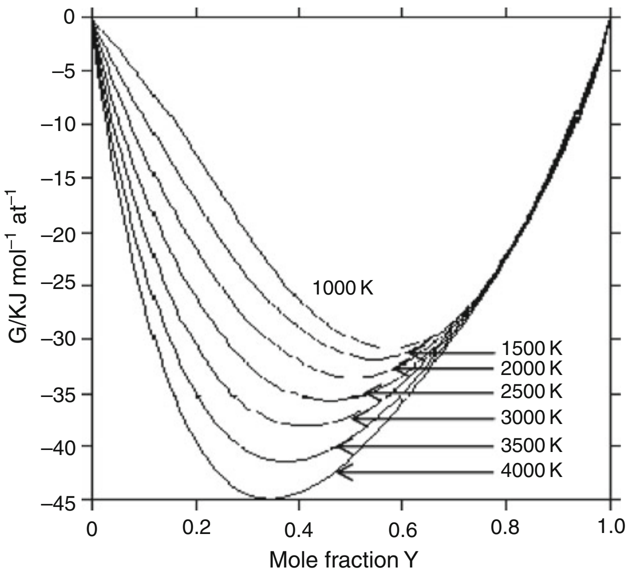

Fig. 6 Gibbs energy of mixing of the liquid phase at different temperature. The reference states were Ru and Y liquids

high temperatures and the terminal solid phase BCC_A2 (βY) is calculated (see Fig. 4).

The calculated and the available experimental values of the enthalpies of formation are listed in Table 4 and presented in Fig. 5. A satisfactory agreement, except for Ru_2Y_3 and $Ru_{25}Y_{44}$ phases for which a maximum of discrepancies of 4.35 kJ mol^{-1} at^{-1}, is noted. The evolutions of Gibbs energy for the liquid phase as a function of temperature (T) are shown in Fig. 6. With our optimization, when T is increasing up to 4000 K, the Gibbs energy for the liquid phase decreases.

Conclusions

A consistent set of thermodynamic parameters were optimized for the different phases of the Ru–Y system. The computed values are in satisfactory agreement with the experimental data for this system, phase diagram data as well as thermodynamic properties. Further experimental determinations, in particular the enthalpy of mixing of the liquid phase, will be necessary to refine the present assessment.

References

1. Idbenali M, Servant C, Selhaoui N, Bouirden L. Thermodynamic assessment of the Ru–Zr binary system. J Phase Equilib. 2007;26:243–9.
2. Kaufman L, Bernstein H. Computer calculations of phase diagrams. New York, NY: Academic Press; 1970.
3. Savitsky EM, Polyakova VP, Roshan NR. The Ru–Y phase diagram. Russ Metall (Engl. Transl.). 1972;5:97–8.
4. Sharifrazi P, Mohanty RC, Raman A. Intermediate phases in some rare earth-ruthenium systems. Z Metallkd. 1984;75:801–5.
5. Fonasini ML, Mugnoli A, Paenzona A. Crystal structure of $Y_{44}Ru_{25}$. J Less-Common Met. 1989;154:149–56.
6. Massalski TB, Okamoto H, Subramanian PR, Kacprzak L. Binary alloy phase diagrams. 2nd ed. Materials Park, OH: ASM; 1990.
7. Selhaoui N, Kleppa OJ. Standard enthalpies of formation of yttrium alloys, Y–Me (Me = Ru, Rh, Pd, Os, Ir, Pt), by high-temperature calorimetry. J Chim Phys. 1993;90:435–43.
8. Selhaoui N, Kleppa OJ. Standard enthalpies of formation of scandium alloys, Sc+Me (Me = Fe, Co, Ni, Ru, Rh, Pd, Ir, Pt), by high-temperature calorimetry. J Alloys Compd. 1993;191:145–9.
9. Selhaoui N, Charles J, Kleppa OJ, Bouirden L, Gachon JC. The Ruthenuim-Yttrium system: an experimental calorimetric study with a phase diagram optimization. J Solid State Chem. 1998; 138:302–6.
10. Charles J, Gachon JC, Hertz J. Different ways to find the thermodynamic functions describing the formation of binary alloys. Part 2. Numerical phase diagram description coupled with experimental measurements. CALPHAD. 1985;9:35–42.
11. Charles J, Notin M, Rahmane M, Hertz J. NANCYUN: a laboratory tool for calculation of binary systems. J Phase Equilib. 1992;13:497–506.
12. Sundman B, Jansson B, Andersson JO. The Thermo-Calc databank system. CALPHAD. 1985;9:153–90.
13. Dinsdale AT. SGTE data for pure elements. CALPHAD. 1991; 15:317–425.
14. Redlich O, Kister A. Algebraic representation of thermodynamic properties and the classification of solutions. Ind Eng Chem. 1948;40:345–8.
15. Chen SL, Daniel S, Zhang F, Chang YA, Oates WA, Schmid-Fetzer R. On the calculation of multicomponent stable phase diagrams. J Phase Equilib. 2001;22:373–8.
16. Arroyave R, Liu ZK. Thermodynamic modelling of the Zn–Zr system. CALPHAD. 2006;30:1–13.
17. Kumar KC, Wollants P. Some guidelines for thermodynamic optimisation of phase diagrams. J Alloys Compd. 2001;320: 189–98.